Published in final edited form as:
Neuropharmacology. 2007 January ; 52(1): 92–99. doi:10.1016/j.neuropharm.2006.05.022.

Differential redistribution of native AMPA receptor complexes following LTD induction in acute hippocampal slices

David Holman, **Marco Feligioni**, and **Jeremy M. Henley***
MRC Centre for Synaptic Plasticity, Department of Anatomy, School of Medical Sciences, University of Bristol, Bristol BS8 1TD, UK

Abstract

AMPAR trafficking is crucial for the expression of certain forms of synaptic plasticity. Here, using surface biotinylation of hippocampal slices and subsequent synaptosome isolation we assessed AMPAR surface expression in synaptosomes following NMDA-evoked long-term depression (NMDA-LTD). Surface levels of GluR1, GluR2 and GluR3 in synaptosomes were markedly reduced 90 min after NMDA-LTD induction. Consistent with endocytosis and degradation, whole-cell surface and total expression levels of GluR2 and GluR3 were also reduced. In contrast, whole-cell surface levels of GluR1 were unaltered at 90 min suggesting that AMPARs with different subunit composition are redistributed to different non-synaptic compartments following LTD induction in acute hippocampal slices.

Keywords

AMPA receptor; NMDA receptor; Long-term depression; Synaptosome; Hippocampal slice; Dendritic spine; AMPAR surface expression; Synapse

1. Introduction

α-Amino-3-hydroxy-5-methyl-4-isoxazole propionic acid receptors (AMPARs) are responsible for most fast excitatory neurotransmission in the mammalian central nervous system and their regulation directly controls synaptic efficacy (Palmer et al., 2005). There are four different AMPAR subunits, GluR1–4, which assemble as tetramers (Greger et al., 2003). The subunit composition of AMPARs is critical in determining the functional and trafficking properties of resulting channels (Malinow and Malenka, 2002). GluR2-containing AMPARs have low Ca^{2+} permeability and consequently display outwardly rectifying current–voltage (I–V) relationships, whereas GluR2-lacking AMPARs have high Ca^{2+} permeability and are inwardly rectifying (Hollmann et al., 1991; Burnashev et al., 1992). In hippocampal neurons AMPARs comprise mainly GluR2 (Ozawa and Lino, 1993) with either GluR1 (GluR1/2) or GluR3 (GluR2/3), although there is evidence for GluR1 homomers and GluR2-lacking heteromers (Wenthold et al., 1996). Based on experiments using recombinant subunits it has been proposed that GluR1/2 complexes are driven into synapses during hippocampal long-term potentiation (LTP), whereas GluR2/3 complexes are continuously inserted into synapses regardless of activity (Shi et al., 2001). More recently, it has been reported that native GluR2-lacking AMPARs are transiently incorporated into synapses during hippocampal LTP, which are later replaced by GluR2-

*Corresponding author. Tel.: +44 117 954 6449; fax: +44 117 929 1687. j.m.henley@bris.ac.uk (J.M. Henley)..

Europe PMC Funders Author Manuscripts

containing receptors (Plant et al., 2006). The rules regulating synaptic AMPAR trafficking during the inverse process of long-term depression are, however, less well defined.

Low frequency stimulation (LFS) is typically used to induce LTD in acute hippocampal slices (Dudek and Bear, 1993) although prolonged synaptic depression can also be evoked by bath application of NMDA (3 min, 20 μM; (Lee et al., 1998)). By mimicking NMDA-LTD in dispersed neuronal culture, several studies have provided valuable insight into the mechanisms of NMDA-induced AMPAR trafficking (Beattie et al., 2000; Ehlers, 2000; Ashby et al., 2004; Lee et al., 2004). As yet, it is unclear how these processes correlate with LTD in slices that, from electrophysiological studies, are considered a more physiologically relevant preparation than dispersed cell cultures.

Using acute hippocampal slices, we have assessed the effects of NMDA-LTD induction on the surface localisation of native GluR1, GluR2 and GluR3. We show that all three subunits are removed from the surface of synaptosomes following NMDA-LTD induction. Interestingly, whole-cell surface and total levels of GluR1 are unaltered under these conditions. In contrast, whole-cell surface and total levels of GluR2 and GluR3 are reduced suggesting that AMPARs with different subunit composition are redistributed to different non-synaptic sites during LTD.

2. Methods

2.1. Electrophysiology

Hippocampal slices (400 μm) were prepared from P21 to 23 male Wistar rats in ice-cold artificial cerebrospinal fluid (ACSF; composition in mM: 124 NaCl; 3 KCl; 26 $NaHCO_3$; 1.25 NaH_2PO_4; 2 $CaCl_2$; 1 $MgSO_4$; 10 D-glucose; saturated with 95% O_2 and 5% CO_2). After removing the CA3 region, slices were transferred to a submersion storage chamber where they were maintained in ACSF for 1 h at room temperature. Field excitatory post-synaptic potentials (*f*EPSPs) were measured at 28 °C using glass recording electrodes filled with ACSF. *f*EPSPs were evoked in the CA1 region by stimulating Schaffer collaterals with 0.2 ms pulses delivered using two bipolar stimulating electrodes. Baseline responses were collected by stimulating once every 15 s using a stimulating intensity of 20 μA. The stimulating intensity was then reduced (5–15 μA) so that the *f*EPSP peak amplitude was 70% of the value obtained using a 20 μA stimulating intensity. LTD was evoked by transient NMDA application (5 min; 20 μM in ACSF; Tocris). *f*EPSPs were recorded for at least 3 h after NMDA treatment. Analysis was performed using the LTP221p Reanalysis computer programme (Anderson and Collingridge, 2001). *f*EPSP slope and fibre volley peak amplitude values were then imported into Sigmaplot where they were normalised against the initial 40 min baseline. Data recorded 10 min before drug treatment and 90 min after drug treatment were compared using paired Student's *t*-tests.

2.2. Slice treatment for biochemical analysis

To compare multiple NMDA- and ACSF (control)-treated slices simultaneously we used a two-chamber perfusion system. Before treating the slices the cortex was removed leaving the CA1/CA2 region. Four to seven slices per group (groups of seven slices were necessary for synaptosome isolation) were equilibrated at room temperature for 1 h before being placed into the chambers of the two-chamber perfusion system (maintained at 28 °C). Following ACSF perfusion for 40 min, one chamber was perfused with ACSF plus 20 μM NMDA for 5 min, while the other chamber was perfused with ACSF alone. Both sets of slices were then perfused with ACSF for a further 15–90 min prior to biochemical analysis.

2.3. Slice biotinylation and homogenisation

Slices were washed once with ice-cold ACSF (5 min) and then incubated with Sulfo-NHS-SS-Biotin (Pierce; 0.5 mg/ml in ACSF) for 30 min on ice. Excess biotin was removed by two brief washes with 50 mM NH_4Cl (in ACSF) and two ACSF washes. Slices were then homogenised in 1 ml of homogenisation buffer (320 mM sucrose; 10 mM Tris; pH 7.4) and centrifuged at 1000 *g* for 5 min to remove nuclear material and cell debris.

2.4. Isolation of hippocampal synaptosomes

Post-nuclear supernatants were layered onto discontinuous step gradients consisting of 20, 10, 6 and 2% percoll (diluted in homogenisation buffer). Purified synaptosomes were collected from the 20–10% percoll interface following 5 min of centrifugation at 35,000 *g* (Nakamura et al., 1993; Grilli et al., 2004). Synaptosomes were then resuspended in 500 μl of lysis buffer (150 mM NaCl, 20 mM HEPES, 2 mM EDTA, 1% Triton, 0.1% SDS, pH 7.4), sonicated and placed on a head-over-head shaker for 2 h. Samples were cleared at 16,000 *g* for 20 min and the protein concentration of the resulting supernatant was determined using a BCA kit (Pierce). Protein matched samples were then used for streptavidin pull downs.

2.5. Isolation of post-synaptic density

Synaptosomes were pelleted by centrifugation (16,000 *g*; 5 min; 4 °C) and resuspended in 300 μl 0.32 M sucrose and 0.1 mM $CaCl_2$. The synaptosomes were then diluted 1:10 in ice-cold 0.1 mM $CaCl_2$ and mixed with an equal volume of 2 × solubilisation buffer (2% Triton X-100, 40 mM Tris, pH 6.0). Following 30 min incubation at 4 °C the insoluble material (synaptic junctions) was pelleted by centrifugation (40,000 *g*, 30 min, 4 °C). The pellet was resuspended in 10 volumes of 1 × solubilisation buffer (1% Triton X-100, 20 mM Tris, pH 8.0) and incubated for 30 min at 4 °C. The suspension was then centrifuged at 40,000 *g* for 30 min at 4 °C. The pellet contained the insoluble post-synaptic density (Phillips et al., 2001).

2.6. Isolation of hippocampal membranes

Post-nuclear supernatants were centrifuged at 100,000 *g* for 1 h and supernatants were discarded. The hippocampal cell membranes were resuspended in 1 ml of lysis buffer, sonicated and then treated as above.

2.7. Streptavidin pull down

Streptavidin beads (40 μl; Sigma) were washed three times with lysis buffer. Lysed biotinylated samples were added to the beads (50 μg total protein) and mixed on a head-over-head shaker for 4 h. Beads were then centrifuged at 800 *g* and the supernatants removed. Beads were subsequently washed three times with lysis buffer and biotinylated proteins were eluted from the beads using 2× SDS-PAGE loading buffer (containing β-mercaptoethanol) at 90 °C for 5 min. The beads were then vortexed for 10 s and centrifuged at 16,000 *g*. Supernatants were removed and stored at −20 °C until further use.

2.8. Quantitative immunoblotting

Proteins were resolved by SDS-PAGE and immunoblotting was performed using a rabbit polyclonal antibody to GluR1 (Upstate; 0.6 μg/ml) and mouse monoclonal antibodies to GluR2 (Chemicon; 1 μg/ml), GluR3 (Chemicon; 2 μg/ml), β-actin (Sigma 0.5 μg/ml), β-tubulin (Sigma; 0.5 μg/ml) and *N*-Cadherin (BD Transduction Laboratories; 1 μg/ml). Quantitative densitometric analysis was performed using NIH Image J.

2.9. Calculation of AMPAR subunit surface expression

Increasing amounts (3.13, 6.25, 12.5, 25 and 50 μg) of total protein were resolved alongside the streptavidin bead-bound and un-bound fractions. Following Western blot analysis, optical density values were obtained for each of the bands representing the input and bound fractions. By plotting these values the percentage surface expression of each subunit was determined by normalising the bound optical band density value to the input band density values. To quantify NMDAR-evoked changes in subunit expression (surface and total) the optical density value of the band representing the NMDA-treated slices was divided by the optical density value of the band representing the ACSF-treated slices. Pooled ACSF band density values were expressed as 1 and pooled NMDA-treated band density values were expressed relative to 1 (±SEM). Statistical analysis was performed using paired Student's *t*-tests.

3. Results and discussion

Crude synaptosome preparations have been used previously to study the synaptic localisation of AMPARs during synaptic plasticity (Heynen et al., 2000). However, it has since emerged that a considerable proportion of GluR2/3 complexes are stored in non-surface, synaptically localised membrane compartments (Lee et al., 2001). Because of this we reasoned that it would be more informative to assess AMPAR expression at the surface of synaptosomes. By biotinylating acute hippocampal slices and subsequently isolating synaptosomes we monitored the surface-synaptosomal expression of AMPARs following LTD induction.

3.1. Surface expression of AMPARs in acute hippocampal slices

First we assessed the whole-cell surface expression of GluR1, GluR2 and GluR3 using biotinylation/streptavidin pull down assays (Thomas-Crusells et al., 2003). GluR4 was not investigated since the expression level of this subunit dramatically decreases beyond post-natal age 14 (Zhu et al., 2000). Increasing proportions of input were resolved alongside 100% of the streptavidin bead-bound and unbound fractions (see Section 2). The whole-cell surface expression of GluR1, GluR2, and GluR3 was in the range 66–78% (Fig. 1A, B). Interestingly, lower levels of GluR2 surface expression have been reported using dispersed hippocampal/cortical neurons (Greger et al., 2002). This apparent difference between tissue preparations may be attributable to higher levels of spontaneous firing in dispersed neuronal cultures (Noel et al., 1999). Elevated levels of spontaneous activity could result in increased activity-dependent internalisation of GluR2 and lower GluR2 surface expression.

We validated the biotinylation protocol by re-probing blots with an antibody to the intracellular protein β-tubulin. As expected, β-tubulin was present exclusively in the unbound fraction (Fig. 1A) indicating that only surface proteins were biotinylated.

3.2. Surface expression of AMPARs in synaptosomes

Next we validated the synaptosome isolation procedure by examining the relative enrichment of various marker proteins. The synaptic markers synaptotagmin and PSD-95 were both enriched in the synaptosome fraction compared to the whole-cell membrane fraction. GluR1 was also enriched in the synaptic fraction, whereas the ER marker calreticulin was predominantly in the whole-cell membrane fraction (Fig. 2A). On further analysis it was evident that AMPARs were markedly enriched in the PSD fraction compared to the total-synaptosomal membrane fraction (Fig. 2B) but it is important to note that not all AMPARs present in synaptosomes are synaptic. Interestingly, the surface expression of GluR1, GluR2 and GluR3 in synaptosomes was in the range 38–62% (Fig. 2C, D). These values are lower than what was estimated for the whole-cell AMPAR population and we

attribute this difference to: (i) a proportion of AMPARs trafficked to the vicinity of the synapse are in a non-surface pool (Lee et al., 2001) and (ii) there is likely to be some contamination of the synaptosome fraction by non-synaptic intracellular organelles. The percentage of GluR3 in the surface fraction was particularly low, which is consistent with a previous report that a large proportion of GluR2/3 complexes are present in sub-synaptic membrane compartments (Lee et al., 2001).

3.3. NMDA-LTD induction reduces the surface expression of GluR1, GluR2 and GluR3 in synaptosomes

Before monitoring the synaptosomal surface expression of AMPAR subunits following LTD induction we confirmed that transient NMDA application induces robust LTD (Lee et al., 1998) in acute hippocampal slices from adolescent rats (P21–23). Field excitatory post-synaptic potentials (*f*EPSPs) were recorded from the CA1 region and changes in basal transmission were monitored. Following 40 min basal transmission, bath application of NMDA (20 μM; 5 min) transiently abolished the *f*EPSP slope (Fig. 3A, B). The *f*EPSP slope partially recovered and stabilised to a level 35–40% less than baseline (Fig. 3A, B, $n = 5$). This LTD induced by 5 min NMDA was not associated with a change in the *f*EPSP fibre volley (Fig. 3C, $n = 5$) indicating that there was no long-term change in pre-synaptic fibre activation. There was no run down in basal transmission in the absence of NMDA. The *f*EPSP slope and fibre volley amplitude were both constant for 160 min (Fig. 3D–F; $n = 3$).

The synaptosomal surface expression of GluR1, GluR2 and GluR3 was assessed at 90 min following NMDA-LTD induction. A significant decrease was observed in the surface levels of all three subunits in synaptosomes from the NMDA-treated slices compared to control (Fig. 3G, H; GluR1 = 0.63 ± 0.10; GluR2 = 0.49 ± 0.08; GluR3 = 0.61 ± 0.08). Similarly, a marked decrease was observed for total-synaptosomal (surface plus intrasynaptosomal) levels of GluR1, GluR2 and GluR3 in the NMDA-treated slices compared to control (Fig. 3G, I; GluR1 = 0.86 ± 0.05; GluR2 = 0.63 ± 0.11; GluR3 = 0.69 ± 0.04).

Since the majority of hippocampal AMPA receptors are thought to be GluR1/2 or GluR2/3 heteromers (Wenthold et al., 1996), our data suggest that both of these receptor complexes are removed from the surface of synapses during LTD. This is consistent with a previous study in which exogenous GluR2 homomers, which have trafficking properties similar to endogenous GluR2/3 heteromers, were removed from synapses following LTD induction in organotypic slice culture (Seidenman et al., 2003). Taken together, our findings suggest that a reduction in the synaptosomal surface localisation of native AMPARs could contribute to LTD expression in acute hippocampal slices.

The mechanisms by which AMPARs are removed from synapses are largely unknown. Nonetheless, evidence suggests that synaptic proteins are endocytosed at sites lateral to the post-synaptic density (Blanpied et al., 2002; Racz et al., 2004). More specifically, it has been reported that NMDA-evoked removal of synaptic AMPARs is preceded by transient endocytosis of extrasynaptic AMPARs in dispersed neuronal culture (Ashby et al., 2004). It is possible therefore that NMDA-LTD induction promotes the untethering of AMPARs from the post-synaptic density allowing for their lateral diffusion to extrasynaptic sites where they are endocytosed.

3.4. NMDA-LTD induction causes differential redistribution of AMPAR subunits

To gain insight into the trafficking events of the total AMPAR pool we assessed the whole-cell surface and total expressed levels of these subunits at 90 min following NMDA-LTD induction. Interestingly, the surface/total expression of GluR1 was unaltered at this time point (Fig. 4A, B; 1.09 ± 0.10 and Fig. 4A, C; 1.04 ± 0.05, respectively; $n = 3$, $p < 0.05$),

whereas at the earlier time of 15 min the surface (but not total) expression of GluR1 was reduced (Fig. 4D–F; 0.82 ± 0.06 and 0.93 ± 0.04; $n = 5$, $p < 0.05$). Our results for GluR1 following NMDA-LTD induction in hippocampal slices are broadly consistent with previous studies that show AMPAR internalisation is enhanced following transient NMDAR activation in dispersed neuronal culture (Ehlers, 2000; Lee et al., 2004). We propose that following NMDA-LTD induction in slices, GluR1 containing AMPARs laterally diffuse away from the PSD, are endoctosed at sites close to the PSD and are then recycled back to non-synaptic surface locations.

In contrast to GluR1, the whole-cell surface and total levels of GluR2 and GluR3 were markedly reduced at 90 min following NMDA-LTD induction (Fig. 4A, C; Surface R2 = 0.80 ± 0.02; R3 = 0.83 ± 0.0004; Total R2 = 0.87 ± 0.02; R3 = 0.74 ± 0.05, $n = 3$, $p < 0.05$). It is likely therefore that GluR2/3 complexes are first internalised and then degraded following NMDA-LTD induction in acute hippocampal slices. Consistent with this, the surface levels of GluR2 and GluR3 were reduced 15 min following NMDA-LTD induction (Fig. 4D, E; GluR2 = 0.71 ± 0.05; GluR3 = 0.72 ± 0.04, $n = 5$, $p < 0.05$), while the total levels of these subunits were unaltered (Fig. 4D, F; GluR2 = 0.90 ± 0.08; GluR3 = 0.97 ± 0.09; $n = 5$; $p > 0.05$). These data are consistent with the report that NMDAR activation promotes AMPAR internalisation and degradation of GluR2 and GluR3 in dispersed neuronal cultures (Lee et al., 2004). We propose that the global loss of GluR2/3 complexes by these processes is a mechanism by which synaptic depression is maintained during the later stages of LTD.

We show that AMPARs with different subunit composition respond differently following NMDA-LTD induction in acute hippocampal slices. It is possible that this differential targeting is mediated by complex-specific accessory protein interactions. For example, synapse associated protein 97 (SAP97) interacts specifically with GluR1 and GluR2-containing AMPARs (Sans et al., 2001) so could mediate the redistribution of GluR1/2 complexes to surface, non-synaptic sites following NMDA-LTD induction. GluR3 containing AMPARs, on the other hand, do not interact with SAP97 (Sans et al., 2001) so could be trafficked elsewhere by GluR3-specific accessory proteins. Future studies will no doubt identify more complex-specific accessory proteins that will likely regulate the differential AMPAR redistribution we observe. Furthermore, it will be interesting to learn what the role of PICK1, GRIP and stargazin are in these processes and how receptor phosphorylation influences the distribution between synaptic and non-synaptic locations.

In conclusion, we have shown that AMPARs containing GluR1, GluR2 or GluR3 are removed from the surface of synaptosomal membranes following LTD induction and provide evidence to suggest that GluR1 containing AMPARs may be redistributed to non-synaptic surface locations during LTD. Finally, we show that LTD induction reduces the synaptosomal, surface and total expressed levels of GluR2 and GluR3 suggesting that surface loss and degradation of these subunits may provide a mechanism by which LTD is maintained.

Acknowledgments

DH is a post-doctoral fellow supported by the EU (GRIP-PANT, PL 005320). We also thank the MRC, the Wellcome Trust and the EU (ENINET LSHM-CT-2005-019063) for financial assistance. We are grateful to B. Johnson, Z. Bashir, P. Matthews, T. Bouschet, P. Hastie, Y. Nakamura, for helpful advice and to D. Rocca, S. Martin, F. Jaskolski, V. Collett, O. Wiegert and S. Kantamneni for constructive reading of the manuscript. We dedicate this paper to the late Dr Werner Hoch who provided invaluable advice and support in the early stages of the work.

Abbreviations

AMPAR	α-Amino-3-hydroxy-5-methyl-4-isoxazole propionic acid receptors
LTD	long-term depression
NMDA	*N*-methyl-D-aspartate
I–V	current–voltage
LTP	long-term potentiation
ACSF	artificial cerebral spinal fluid
***f*EPSP**	field excitatory post-synaptic potential

References

Anderson WW, Collingridge GL. The LTP program: a data acquisition program for on-line analysis of long-term potentiation and other synaptic events. Journal of Neuroscience Methods. 2001; 108:71–83. [PubMed: 11459620]

Ashby MC, De La Rue SA, Ralph GS, Uney J, Collingridge GL, Henley JM. Removal of AMPA receptors (AMPARs) from synapses is preceded by transient endocytosis of extrasynaptic AMPARs. Journal of Neuroscience. 2004; 24:5172–5176. [PubMed: 15175386]

Beattie EC, Carroll RC, Yu X, Morishita W, Yasuda H, von Zastrow M, Malenka RC. Regulation of AMPA receptor endocytosis by a signaling mechanism shared with LTD. Nature Neuroscience. 2000; 3:1291–1300.

Blanpied TA, Scott DB, Ehlers MD. Dynamics and regulation of clathrin coats at specialized endocytic zones of dendrites and spines. Neuron. 2002; 36:435–449. [PubMed: 12408846]

Burnashev N, Monyer H, Seeburg PH, Sakmann B. Divalent ion permeability of AMPA receptor channels is dominated by the edited form of a single subunit. Neuron. 1992; 8:189–198. [PubMed: 1370372]

Dudek SM, Bear MF. Bidirectional long-term modification of synaptic effectiveness in the adult and immature hippocampus. Journal of Neuroscience. 1993; 13:2910–2918. [PubMed: 8331379]

Ehlers MD. Reinsertion or degradation of AMPA receptors determined by activity-dependent endocytic sorting. Neuron. 2000; 28:511–525. [PubMed: 11144360]

Greger IH, Khatri L, Ziff EB. RNA editing at arg607 controls AMPA receptor exit from the endoplasmic reticulum. Neuron. 2002; 34:759–772. [PubMed: 12062022]

Greger IH, Khatri L, Kong X, Ziff EB. AMPA receptor tetramerization is mediated by Q/R editing. Neuron. 2003; 40:763–774. [PubMed: 14622580]

Grilli M, Raiteri L, Pittaluga A. Somatostatin inhibits glutamate release from mouse cerebrocortical nerve endings through presynaptic sst2 receptors linked to the adenylyl cyclase-protein kinase A pathway. Neuropharmacology. 2004; 46:388–396. [PubMed: 14975694]

Heynen AJ, Quinlan EM, Bae DC, Bear MF. Bidirectional, activity-dependent regulation of glutamate receptors in the adult hippocampus in vivo. Neuron. 2000; 28:527–536. [PubMed: 11144361]

Hollmann M, Hartley M, Heinemann S. Ca^{2+} permeability of KA-AMPA – gated glutamate receptor channels depends on subunit composition. Science. 1991; 252:851–853. [PubMed: 1709304]

Lee HK, Kameyama K, Huganir RL, Bear MF. NMDA induces long-term synaptic depression and dephosphorylation of the GluR1 subunit of AMPA receptors in hippocampus. Neuron. 1998; 21:1151–1162. [PubMed: 9856470]

Lee SH, Simonetta A, Sheng M. Subunit rules governing the sorting of internalized AMPA receptors in hippocampal neurons. Neuron. 2004; 43:221–236. [PubMed: 15260958]

Lee SH, Valtschanoff JG, Kharazia VN, Weinberg R, Sheng M. Biochemical and morphological characterization of an intracellular membrane compartment containing AMPA receptors. Neuropharmacology. 2001; 41:680–692. [PubMed: 11640922]

Malinow R, Malenka RC. AMPA receptor trafficking and synaptic plasticity. Annual Review of Neuroscience. 2002; 25:103–126.

Nakamura Y, Iga K, Shibata T, Shudo M, Kataoka K. Glial plasmalemmal vesicles – a subcellular fraction from rat hippocampal homogenate distinct from synaptosomes. Glia. 1993; 9:48–56. [PubMed: 7902337]

Noel J, Ralph GS, Pickard L, Williams J, Molnar E, Uney JB, Collingridge GL, Henley JM. Surface expression of AMPA receptors in hippocampal neurons is regulated by an NSF-dependent mechanism. Neuron. 1999; 23:365–376. [PubMed: 10399941]

Ozawa S, Lino M. Two distinct types of AMPA responses in cultured rat hippocampal neurons. Neuroscience Letters. 1993; 155:187–190. [PubMed: 7690918]

Palmer CL, Cotton L, Henley JM. The molecular pharmacology and cell biology of {alpha}-amino-3-hydroxy-5-methyl-4-isoxazolepropionic acid receptors. Pharmacological Review. 2005; 57:253–277.

Phillips GR, Huang JK, Wang Y, Tanaka H, Shapiro L, Zhang W, Shan WS, Arndt K, Frank M, Gordon RE, Gawinowicz MA, Zhao Y, Colman DR. The presynaptic particle web: ultrastructure, composition, dissolution, and reconstitution. Neuron. 2001; 32:63–77. [PubMed: 11604139]

Plant K, Pelkey KA, Bortolotto ZA, Morita D, Terashima A, McBain CJ, Collingridge GL, Isaac JT. Transient incorporation of native GluR2-lacking AMPA receptors during hippocampal long-term potentiation. Nature Neuroscience. 2006; 9:602–604.

Racz B, Blanpied TA, Ehlers MD, Weinberg RJ. Lateral organization of endocytic machinery in dendritic spines. Nature Neuroscience. 2004; 7:917–918.

Sans N, Racca C, Petralia RS, Wang YX, McCallum J, Wenthold RJ. Synapse-associated protein 97 selectively associates with a subset of AMPA receptors early in their biosynthetic pathway. Journal of Neuroscience. 2001; 21:7506–7516. [PubMed: 11567040]

Seidenman KJ, Steinberg JP, Huganir R, Malinow R. Glutamate receptor subunit 2 Serine 880 phosphorylation modulates synaptic transmission and mediates plasticity in CA1 pyramidal cells. Journal of Neuroscience. 2003; 23:9220–9228. [PubMed: 14534256]

Shi S, Hayashi Y, Esteban JA, Malinow R. Subunit-specific rules governing ampa receptor trafficking to synapses in hippocampal pyramidal neurons. Cell. 2001; 105:331–343. [PubMed: 11348590]

Thomas-Crusells J, Vieira A, Saarma M, Rivera C. A novel method for monitoring surface membrane trafficking on hippocampal acute slice preparation. Journal of Neuroscience Methods. 2003; 125:159–166. [PubMed: 12763242]

Wenthold RJ, Petralia RS, Blahos J II, Niedzielski AS. Evidence for multiple AMPA receptor complexes in hippocampal CA1/CA2 neurons. Journal of Neuroscience. 1996; 16:1982–1989. [PubMed: 8604042]

Zhu JJ, Esteban JA, Hayashi Y, Malinow R. Postnatal synaptic potentiation: delivery of GluR4-containing AMPA receptors by spontaneous activity. Nature Neuroscience. 2000; 3:1098–1106.

Europe PMC Funders Author Manuscripts

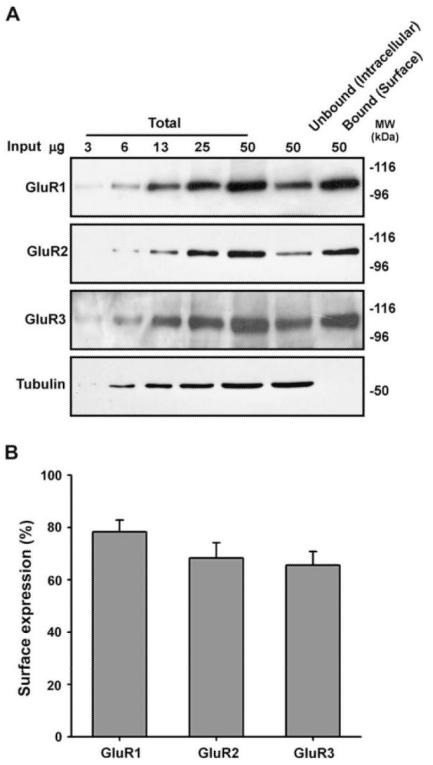

Fig. 1.

AMPA receptor surface expression in hippocampal slices. Acute hippocampal slices from P21 to 23 male Wistar rats were biotinylated and the surface expression of each subunit was determined by quantitative immunoblotting (see Section 2). (A) Representative blots for GluR1, GluR2, GluR3 and β-tubulin. (B) Proportion of AMPAR subunits that are surface expressed (mean ± SEM of three independent experiments).

Europe PMC Funders Author Manuscripts

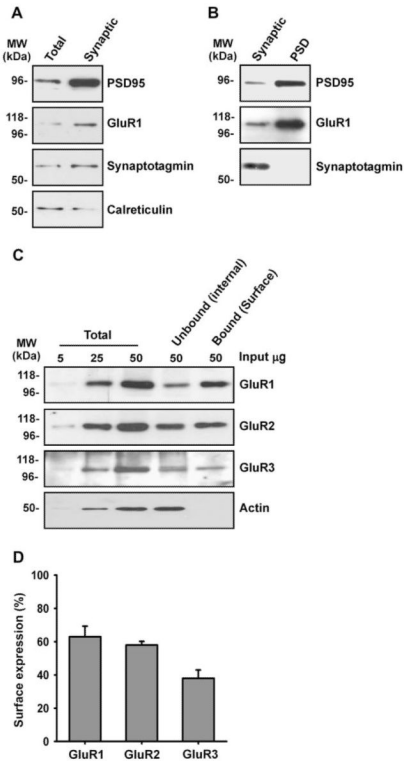

Fig. 2.

Characterisation of synaptosome preparation. Acute hippocampal slices from P21 to 23 male Wistar rats were biotinylated, synaptosomes were isolated and the surface expression of each subunit was determined by quantitative immunoblotting (see Section 2). (A) Synaptotagmin, PSD-95 and GluR1 were enriched in the synaptosome fraction compared to the whole-cell membrane fraction. (B) GluR1 and PSD-95 but not synaptotagmin were enriched in the PSD fraction compared to the synaptosome fraction. (C) Representative blots for GluR1, GluR2, GluR3 and β-actin. (D) Proportion of AMPAR subunits that are surface expressed in synaptosomes (mean ± SEM of three independent experiments).

Europe PMC Funders Author Manuscripts

Europe PMC Funders Author Manuscripts

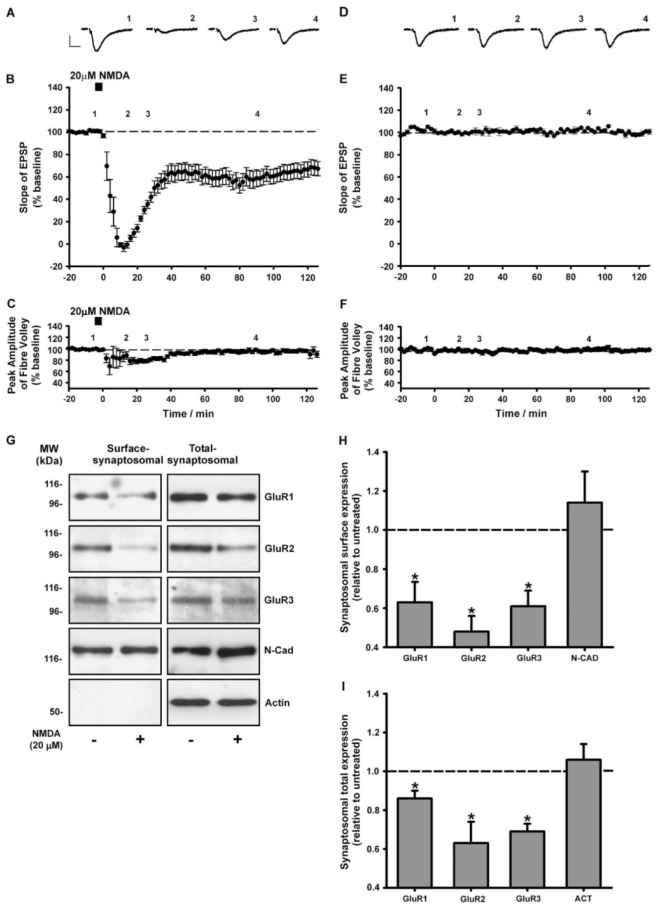

Fig. 3.

Down-regulation of synaptosomal AMPARs 90 min following NMDA-LTD induction. (A) Example traces at $t_1 = -5$, $t_2 = 20$, $t_3 = 30$ and $t_4 = 90$ min (labelled 1–4). (B, C) NMDA application (5 min, 20 μM) causes a prolonged reduction in the *f*EPSP slope. No long-term changes in *f*EPSP fibre volley amplitude were detected. Data represent the mean ± SEM of five independent experiments. (D–F) In the absence of NMDA application no change was observed in the *f*EPSP slope or fibre volley amplitude. Data represent the mean ± SEM of three independent experiments. Example traces (D) represent $t_1 = -5$, $t_2 = 20$, $t_3 = 30$ and $t_4 = 90$ min. Calibration bars 10 ms, 0.5 mV. (G) Representative blots for surface-synaptic and total-synaptic GluR1, GluR2 and GluR3. There were significant decreases in the levels of surface-synaptosomal (H) and total-synaptosomal (I) GluR1, GluR2 and GluR3 in the NMDA-treated slices compared to control. No change was observed in the levels of surface-synaptosomal N-cadherin or total-synaptosomal β-actin. Data represent the mean ± SEM of at least four independent experiments (*$P < 0.05$).

Europe PMC Funders Author Manuscripts

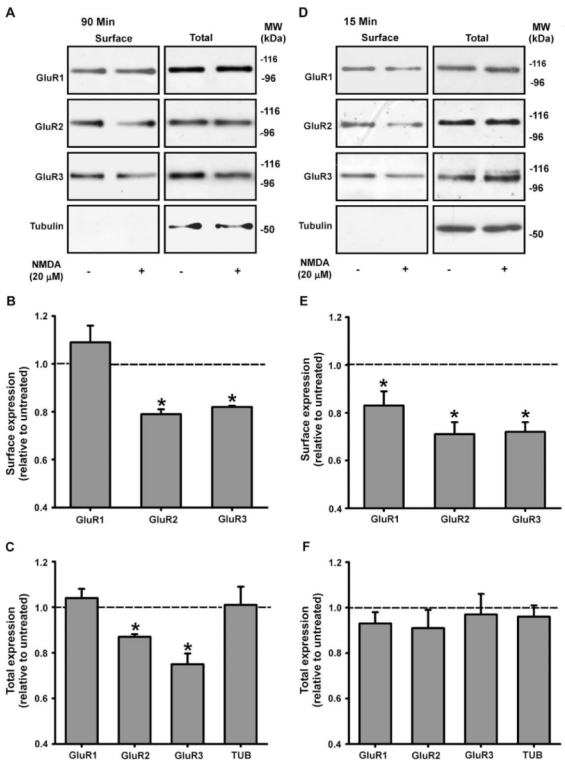

Fig. 4.

Subunit specific reduction in whole-cell surface and total expression 90 min following NMDA-LTD induction. (A, D) Representative blots for whole-cell surface and total AMPAR subunits at 15 and 90 min. (B, C) At 90 min there were significant decreases in the surface and total levels of GluR2 and GluR3 in the NMDA-treated slices compared to control. No significant differences were detected for GluR1 at 90 min. At 15 min there were significant decreases in the levels of surface, but not total, GluR1, GluR2 and GluR3 in the NMDA-treated slices compared to control (D–F). No differences were detected for β-tubulin at 15 or 90 min. Data represent the mean ± SEM of at least three independent experiments (*$P < 0.05$).